J. Biochem. **142,** 655–661 (2007)
doi:10.1093/jb/mvm180

Spectrally and Time-resolved Fluorescence Spectroscopic Study on Melittin–Calmodulin Interaction

Takuhiro Otosu, Etsuko Nishimoto and Shoji Yamashita*

Institute of Biophysics, Faculty of Agriculture, Graduate School of Kyushu University, Hakozaki, Fukuoka 812-8581, Japan

Received June 28, 2007; accepted September 6, 2007; published online September 28, 2007

The origin of multi-exponential fluorescence decay property of tryptophan (Trp) in protein has been in controversy, and dielectric relaxation is thought to be one of the most plausible candidates of that origin. In this study, we studied melittin–calmodulin interaction on the concept of dielectric relaxation by spectrally and time-resolved fluorescence spectroscopy. Trp residue in melittin demonstrated drastic change in its dielectric relaxation rate and scale by binding with calmodulin. Expected change of relaxation rate suggested that dielectric relaxation accounts for multi-exponential property of fluorescence decay. We also examined the time variation of radiative and non-radiative decay rates. That result demonstrated the distinct difference profiles of non-radiative decay rate of Trp in melittin and the complex.

Key words: calmodulin, dielectric relaxation, melittin, TCSPC, time-resolved fluorescence.

Abbreviations: CaM, calmodulin; EDTA, ethylenediaminetetraacetic acid; FWHM, full width at half-maximum; NATA, N-acetyl-l-tryptophanamide; TCA, trichloroacetic acid; TCSPC, time-correlated single photon counting.

Recent development of optical and detection system has strikingly expanded the application of fluorescence spectroscopy to wide range of biological science. Those approaches include fluorescence correlation spectroscopy and fluorescence resonance energy transfer of protein on one molecular level (*1–3*).

In those studies, time-resolved fluorescence spectroscopy combined such advanced technique with basic knowledge and screened out the intra- and intermolecular interaction mechanism on the energy relaxation process. Fluorescence decay kinetics of protein is usually described as linear combination of exponentials, even in single tryptophan (Trp) proteins.

Rationalizing the decay parameters, we can elucidate function–structure relationships of protein by time-resolved fluorescence spectroscopy. But the origin of that multi-exponentiality has been in controversy and this hampers the interpretation of fluorescence data. There are several interpretations about multi-exponential or non-exponential decay of single Trp fluorescence in peptides and proteins (*4–12*). One of those interpretation models is rotamer model that ground state conformation heterogeneity of Trp in protein is responsible for each decay component. Several authors have showed rotamer population identified by NMR corresponded to decay component of fluorophore and some peptides (*5*, *6*).

Dielectric relaxation process during excited state is also a potent factor in multi-exponential decay kinetics of Trp in proteins. Recently, Toptygin *et al*. (*9–12*) have proposed a quantitative fluorescence decay kinetics model based on dielectric relaxation process and showed the data of solvatochromic dye and proteins coincided well with their model. Electrostatic solute–solvent interaction occurred in the energy relaxation process is very important factor in understanding the function–structure correlation especially in protein–protein interaction. That is because change of hydration and electric field around residues in specific domain is anticipated.

In many studies of protein interaction, calmodulin (CaM) has been widely used and a variety of studies including other spectroscopy such as NMR have been done (*13–16*).

CaM is ubiquitous calcium-binding protein, which works as a signal transducer via Ca^{2+} ion in eukaryotic cells. CaM has two domains and each domain binds two Ca^{2+}. By binding with Ca^{2+}, CaM drastically changes its own conformation. It exposes hydrophobic clefts and re-orientates four helices in each domain to bind and activate many target proteins and peptides. Several proteins are known to interact with apo-CaM such as glutamate decarboxylase and melittin (*17*, *18*). Binding mechanism of apo-CaM with target protein is under investigation.

The advantage of using CaM for fluorescence studies is that it has no Trp in its sequence. Therefore, if target protein has Trp residue in its sequence, we can investigate CaM–ligand interaction by analysing Trp fluorescence in the target. Furthermore, Trp residue in CaM interaction domain of many target protein is thought to be one of the anchor residues and key amino acids to understanding the binding versatility of CaM with

*To whom correspondence should be addressed. Tel/Fax: +81-92-642-4425, E-mail: yamashita@brs.kyushu-u.ac.jp

ligand, which is now hot topic in CaM–ligand interaction study (*14*, *15*).

As stated before, changes of hydration, electric field and dielectric relaxation response are very important aspect of protein–protein interaction. So in the present study, we focused on melittin as a target peptide of CaM and investigated those interactions by time-resolved fluorescence spectroscopy using dielectric relaxation model.

MATERIALS AND METHODS

Purification of CaM and Melittin—The purification of CaM was performed by modifying the method of Yazawa *et al*. (*19*). Squash was ground and homogenized in 50 mM sodium phosphate buffer, pH 5.7 including 5 mM EDTA. The formed slurry was stirred for 10 min and centrifuged at 10,000*g* for 30 min at 4°C to extract the crude proteins. Removing insoluble components by filtration, 50% TCA was added to the crude protein solution (final conc. 3%) and adjusted to pH 5.2 by NaOH. After incubation for 1 h, the slurry was centrifuged at 10,000*g* for 30 min Fifty percent of TCA was added to the supernatant (final conc. 6%) and centrifuged at 10,000*g* for 30 min. The precipitated proteins were suspended in 10 mM Tris–HCl and 1 mM EDTA, pH 8.0. Ammonium sulphate was added to the suspension (final conc. 50%) and centrifuged at 17,000*g* for 20 min. Fifty percent of TCA was added to the supernatant (final conc. 7%) and centrifuged at 10,000*g* for 30 min. The precipitated proteins were suspended and dialysed against 50 mM Tris–HCl and 0.1 mM EDTA, pH 8.0. Calcium chloride (0.2 M) was added to the dialysed sample (final conc. 5 mM) and applied to the Phenyl-Sepharose column (GE Healthcare Bio-Science, NJ, USA) previously equilibrated with 50 mM Tris–HCl and 0.1 mM $CaCl_2$, pH 7.5. Bound protein was eluted with 50 mM Tris–HCl, 0.5 M NaCl and 1 mM EGTA, pH 7.5. The peak fraction was collected and dialysed against 50 mM sodium phosphate buffer containing 5 mM EDTA, pH 5.7. The sample was applied to the Sephacryl S-100 column (GE Healthcare Bio-Science, NJ, USA) equilibrated with 50 mM Tris–HCl, 0.2 M NaCl, pH 7.5 and the peak fraction was applied to the UNO-Q column (Bio-Rad, CA, USA) equilibrated with the same buffer. The fraction corresponding to CaM was collected and dialysed against 50 mM Tris–HCl, pH 7.5. Every chromatography was performed on biologic column system (Duo-flow, Bio-Rad, CA, USA) at 4°C.

Melittin was purchased from Sigma and purified with reverse-phase HPLC on Inertsil Peptides C-18 column (GL Sciences, Japan). Melittin is 26-residue polypeptide and possesses one Trp residue at position 19. The purities of CaM and melittin were examined by MALDI-TOF mass spectrometer (Kratos TOF mass spectrometer AXIMA-CFR plus, Shimadzu, Japan).

Steady-State Absorbance Measurements—The steady-state absorption spectra were recorded on Ultraspec 3100 pro spectrophotometer (GE Healthcare Bio-Science, NJ, USA).

Steady-State and Time-Resolved Fluorescence Measurements—For fluorescence measurement, protein concentration was adjusted to under 50 μM by diluting with 50 mM Tris–HCl, pH 7.5. We performed every measurement without Ca^{2+} at 20°C.

The steady-state fluorescence emission spectra were recorded on Hitachi 850 fluorescence spectrophotometer (Hitachi, Tokyo). Excitation wavelength was set to 295 nm. The fluorescence emission spectra were strictly corrected against detection and excitation systems. The undesired effects of stray light were also removed by subtraction.

The time-resolved fluorescence decays of melittin and the complex with CaM were measured with the sub-picosecond laser-based time-correlated single photon counting method (TCSPC) precisely described by Fukunaga *et al*. (*20*). Briefly, excitation pulse (295 nm) was separated from a combination of sub-picosecond Ti:Sapphire laser (Tsunami, Spectra-Physics, CA, USA), pulse picker with second harmonic generator (model 3980, Spectra-Physics, CA, USA) and third harmonic generator (GWU, Spectra-Physics, CA, USA). The repetition rate was 1 MHz and excitation pulse width was 100 fs. The channel width was 10.7 ps/ch. The full width at half-maximum (FWHM) of instrument response function was 86.7 ps. The adequacy of the curve fitting was judged by the residual plots and the statistic parameters such as serial variance ratio (SVR) and sigma value (σ) (*21*).

The dielectric relaxation model was explicitly defined by Toptygin *et al*. (*9*, *11*). In their model, parameters obtained at only one emission wavelength are not meaningful but time variation of the fluorescence centre of gravity has an impact. The time-dependent shift of fluorescence centre of gravity $\bar{\nu}(t)$ was expressed as follows:

$$\bar{\nu}(t) = \frac{\int_0^\infty \nu\left[\nu^{-3} F_\nu(\nu,t)\right]\mathrm{d}\nu}{\int_0^\infty \left[\nu^{-3} F_\nu(\nu,t)\right]\mathrm{d}\nu} \tag{1}$$

$$F_\nu(\nu,t) = \sum_{n=1}^{N\exp} \alpha_n(\nu) \exp\left\{\frac{-t}{\tau_n(\nu)}\right\} \tag{2}$$

where, $F_\nu(\nu,t)$ is the spectrally and time-resolved fluorescence decay. Substituting Eq. 2 into Eq. 1 and changing those parameters into experimental one yields

$$\bar{\nu}(t) = \frac{\sum_{n=1}^{N\exp}\sum_m \lambda_m^2 \alpha_{mn} \exp\{-t/\tau_n(\lambda)\}}{\sum_{n=1}^{N\exp}\sum_m \lambda_m^3 \alpha_{mn} \exp\{-t/\tau_n(\lambda)\}} \tag{3}$$

$$\alpha_{mn} = \alpha_{mn}^{\exp} \frac{F_{ss}(\lambda_m)}{\sum_i \alpha_{mi}\tau_i} \tag{4}$$

λ_m is measurement wavelength; α_{mn} denotes decay amplitude normalized by steady-state fluorescence intensity and F_{ss} represents steady-state fluorescence intensity. The time derivatives of natural logarithm of excited state population ($N(t)$) is defined by

$$-\frac{\partial \ln[N(t)]}{\partial t} = \frac{\sum_{n=1}^{N\exp}\sum_m \lambda^3 \alpha_{mn} \tau_n^{-1}(\lambda) \exp\{-t/\tau_n(\lambda)\}}{\sum_{n=1}^{N\exp}\sum_m \lambda^3 \alpha_{mn} \exp\{-t/\tau_n(\lambda)\}} = k_r + k_{nr} \tag{5}$$

where, k_r and k_{nr} represent radiative and non-radiative decay constants, respectively.

RESULTS AND DISCUSSION

At 10–40°C, the rotational correlation time of the complex was linear with respect to 1/T (data not shown), which indicated no structural change was occurred in that temperature range. So measurement temperature was set to 20°C.

Figure 1 shows steady-state fluorescence and absorption (inset) spectra of melittin and its complex with CaM. The fluorescence intensity of Trp in melittin was enhanced by binding CaM and the peak wavelength shifted to higher energy side (melittin, 356 nm; complex, 339 nm). The peak wavelength and the shape of fluorescence spectra of the complex were same irrespective of Ca^{2+}. Based on the difference of fluorescence spectra between melittin and the complex with CaM, Ca^{2+} effects on the stoichiometry and binding energy were analysed by titration curves. No remarkable effect of Ca^{2+} was also recognized on the formation of melittin–CaM complex.

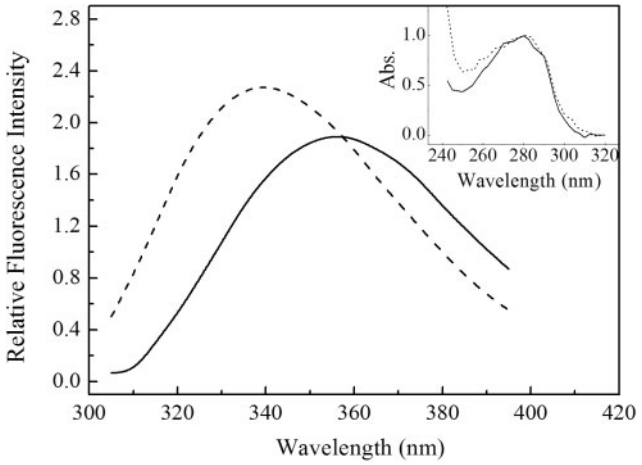

Fig. 1. **Steady-state fluorescence emission spectra of melittin and the complex with CaM.** Excitation wavelength was 295 nm. Solid line, melittin; dashed line, the complex with CaM. Inset, absorption spectra of melittin and the complex with CaM; solid line, melittin; dashed line, the complex with CaM.

Figure 2 showed fluorescence decay curves of melittin and the complex with CaM. Fluorescence decay parameters of melittin and the complex with CaM giving the best fit were shown in Table 1. All of decays were described with a linear combination of triple exponentials. As shown in Fig. 3 and Table 1, average lifetimes (τ_{av}) were increased with increasing emission wavelength in both of samples and this tendency was more remarkable in complex. We did not find any negative pre-exponential factor which was an evidence for involvement of dielectric relaxation process. Actually, negative pre-exponential factor is frequently observed in the case of upconversion study. But it depends on relaxation rate and time window of measurement. If rise time corresponding to dielectric relaxation process was comparable with total decay rate and could not be resolved, decay time would be observed to be longer as a result. Table 1 showed that each lifetime increased with increasing emission wavelength. If conformational heterogeneity exists, each rotamer or conformer give intrinsic lifetime and those lifetimes are independent on emission wavelength. So the fluorescence decay properties of melittin and the complex are consistently rationalized with dielectric relaxation model.

Decay-associated spectra (data not shown) showed that the decay component corresponding to shorter lifetime had emission peak maximum at shorter wavelength in complex. This trend was consistent with the dielectric relaxation model. But, in melittin, intermediate component (τ_2) had slightly longer wavelength than that of longest component (τ_1).

Using the fluorescence decay parameters shown in Table 1, instantaneous spectra and $\bar{\nu}(t)$ of melittin and the complex were calculated. Instantaneous spectra are shown in Fig. 4. Those spectra were both red-shifted by time but the rates and scales of those shifts were distinguishable each other. The FWHMs of the

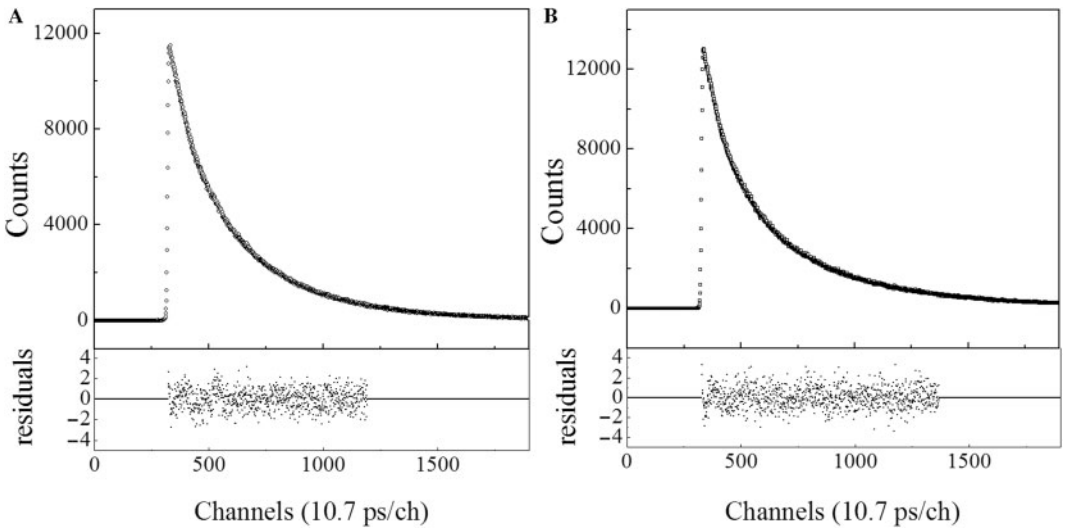

Fig. 2. **Fluorescence decay curves (upper panel) and residuals (lower panel) giving the best fit of melittin (A) and the complex with CaM (B).** Excitation wavelength was 295 nm. Emission wavelength was 355 nm.

Table 1. **Fluorescence decay parameters of melittin and the complex with CaM.**

λ (nm)	α_1	α_2	α_3	τ_1 (ns)	τ_2 (ns)	τ_3 (ns)	τ_{av} (ns)	σ	SVR
Melittin									
320	0.44	0.25	0.30	3.35	0.83	0.13	1.74	1.04	1.95
330	0.51	0.30	0.20	3.58	1.17	0.27	2.22	1.03	2.06
335	0.49	0.31	0.21	3.74	1.40	0.35	2.32	1.12	1.75
340	0.49	0.32	0.19	3.74	1.41	0.32	2.35	1.02	1.95
345	0.51	0.28	0.21	3.56	1.01	0.10	2.12	1.04	1.74
350	0.49	0.31	0.20	3.78	1.40	0.21	2.33	1.04	1.82
355	0.50	0.30	0.20	3.79	1.49	0.28	2.40	0.99	1.79
360	0.49	0.33	0.18	3.90	1.68	0.34	2.54	1.04	2.03
365	0.53	0.29	0.18	3.76	1.50	0.26	2.47	1.09	1.79
370	0.50	0.33	0.17	3.92	1.73	0.33	2.59	1.00	1.87
375	0.49	0.35	0.17	3.94	1.74	0.27	2.56	1.05	1.72
380	0.52	0.34	0.15	3.93	1.79	0.34	2.68	1.07	1.95
390	0.59	0.30	0.11	3.80	1.57	0.31	2.74	1.05	1.94
Complex									
320	0.26	0.46	0.29	4.68	1.63	0.38	2.05	1.01	1.83
325	0.28	0.45	0.27	4.72	1.59	0.35	2.13	1.11	1.82
330	0.29	0.43	0.28	4.77	1.65	0.37	2.21	1.06	1.90
335	0.30	0.42	0.28	4.90	1.70	0.36	2.28	1.01	1.74
340	0.31	0.42	0.27	5.01	1.70	0.35	2.37	1.04	1.83
345	0.32	0.41	0.27	4.84	1.50	0.21	2.24	1.25	1.23
355	0.34	0.42	0.23	5.19	1.68	0.28	2.56	1.07	1.80
360	0.36	0.41	0.23	5.16	1.60	0.22	2.58	1.09	1.66
365	0.37	0.40	0.22	5.24	1.68	0.25	2.69	1.10	1.58
370	0.40	0.41	0.19	5.26	1.68	0.30	2.86	1.03	1.98
375	0.40	0.40	0.19	5.35	1.71	0.26	2.89	1.07	1.78
380	0.40	0.42	0.18	5.46	1.80	0.32	3.00	1.03	2.00
390	0.38	0.44	0.18	5.86	2.00	0.32	3.17	1.01	1.79

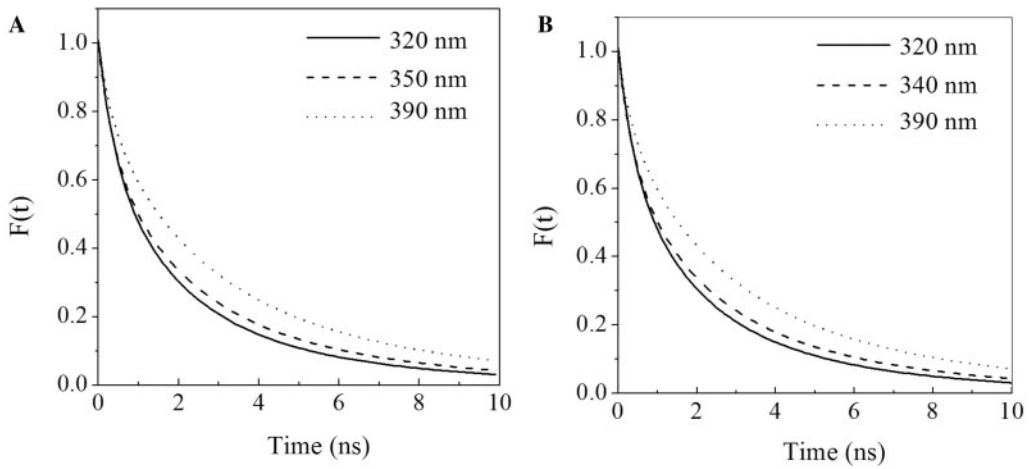

Fig. 3. **Emission wavelength dependence of fluorescence decay curves of melittin (A) and the complex with CaM (B).** Each line was generated by the parameters described in Table 1. Excitation wavelength was 295 nm.

instantaneous spectra were not so changed in both proteins, which was consistent with the relaxation model (data not shown). Because if Trp is in heterogeneity environment, the difference of emission peak wavelengths and lifetimes of each conformation causes the change of FWHMs.

Figure 5 displayed time variation of fluorescence centre of gravity of melittin and the complex. According to Toptygin *et al*. (*9*), $\bar{\nu}(t)$ curves were fitted by a linear combination of exponential function. But, in melittin, large deviation of exponential at $7\,\text{ns} < t < 20\,\text{ns}$ was recognized (Fig. 5 inset) that deviation would probably come from delayed fluorescence or phosphorescence, or just an experimental artefact, so we restricted to these data at $0\,\text{ns} < t < 6\,\text{ns}$ region. These two curves were fitted by two exponentials and constants. Table 2 showed fitting parameter for melittin and the complex. The relaxation rate became much longer by binding with CaM.

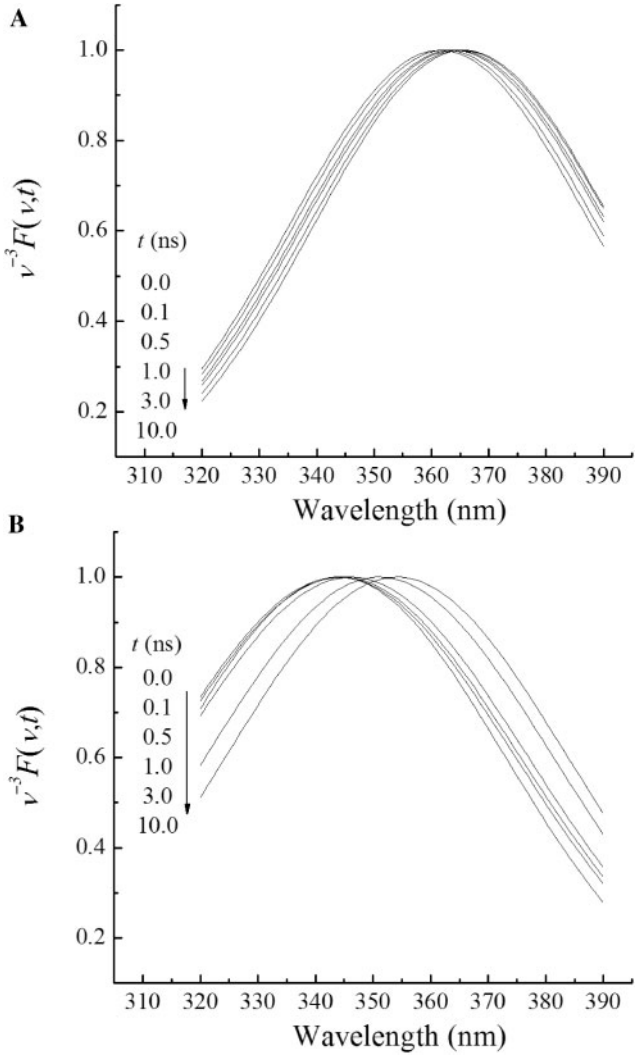

Fig. 4. **Normalized instantaneous emission spectra of melittin (A) and the complex with CaM (B).** These spectra were generated by Gaussian fitting of $\nu^{-3}F_v(v,t)$ of six different t-values. The adequacy of fitting was judged by coefficient of determination and we obtained $R^2 > 0.99$.

Though the crystal structure of the complex are not available, most of Trp in CaM-binding peptides are packed into protein matrix upon binding with CaM. The restricted motion of residues and/or water molecules surrounding Trp in the protein matrix would result in the slowing down of dielectric relaxation of Trp. This reasonable result emphasized the validity of relaxation model. On the other hand, $\bar{\nu}(\infty)$ values were not so different from each other (melittin, 27,900 cm^{-1}; complex, 28,200 cm^{-1}). That indicated that the energy differences between relaxed excited state and ground state of melittin and the complex with CaM were almost the same. This conclusion is hardly derived from steady-state fluorescence spectra shown in Fig. 1, which have peaks at 28,090 cm^{-1} (melittin) and 29,500 cm^{-1} (complex) because steady-state fluorescence spectra of melittin and the complex are time-averaging and greatly dependent on fluorescence lifetime and relaxation rate.

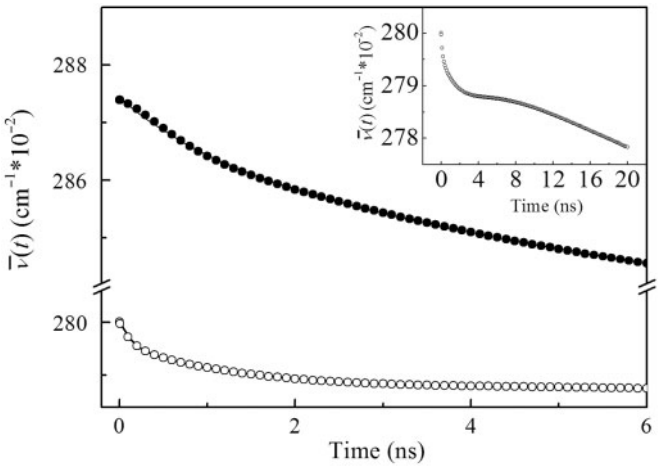

Fig. 5. **Time variation of the center of gravity $\bar{\nu}$ of the instantaneous emission spectra.** The plots in the graph showed $\bar{\nu}$ at arbitrary time calculated by using Eq. 3. Open circles, melittin; filled circles, the complex with CaM. Data were fitted by $\bar{\nu}(t) = \sum \alpha_{ri} \exp(-t/\tau_{ri}) + \bar{\nu}(\infty)$ shown by solid lines. Inset, time variation of the centre of gravity of melittin.

Table 2. **Decay parameters of time variation of the fluorescence centre of gravity.**

	α_{r1}	α_{r2}	τ_{r1} (ns)	τ_{r2} (ns)	$\bar{\nu}(\infty)$ (cm^{-1})	λ (∞) (nm)
Melittin	0.646	0.354	1.39	0.138	27900	358.4
Complex	0.833	0.167	12.05	1.132	28200	354.6

These parameters were obtained by fitting $\bar{\nu}(t)$ curves with $\bar{\nu}(t) = \sum \alpha_{ri} \exp(-t/\tau_{ri}) + \bar{\nu}(\infty)$.

To calculate sum of the radiative and non-radiative decay rates using Eq. 5, we plotted the time derivatives of natural logarithm of excited state population against time (Fig. 6). Time variations of the sum of radiative and non-radiative decay rates were described with a linear combination of double exponentials and constants. As shown in Table 3, fast and slow lifetimes of the complex were longer than that of melittin. On the other hand, the limit of sum of radiative and non-radiative decay rate in the complex was 1.49-fold smaller than that in melittin. The decay curve of the sum of radiative and non-radiative decay rate in melittin was resembled to the curve of the center of gravity. But in complex, time variation of the sum of overall decay rates was different to that of centre of gravity. To investigate whether these differences were attributed to radiative decay rate or non-radiative one, we attempted to calculate the time average of radiative decay rate. By using time integration of Eq. 5 and the parameters shown in Table 3, we described the decay of excited state population of Trp in melittin and the complex (Fig. 7) as following equation

$$\frac{N(t)}{N(0)} = \exp\left[-\left\{k_r(t) + k_{nr}(t)\right\}t\right] = \exp\left[-\left\{\sum \alpha_{ki} \exp(-t/\tau_{ki}) + k_r(\infty) + k_{nr}(\infty)\right\}t\right] \quad (6)$$

We fitted two curves with exponential functions and calculated average lifetime of excited state population

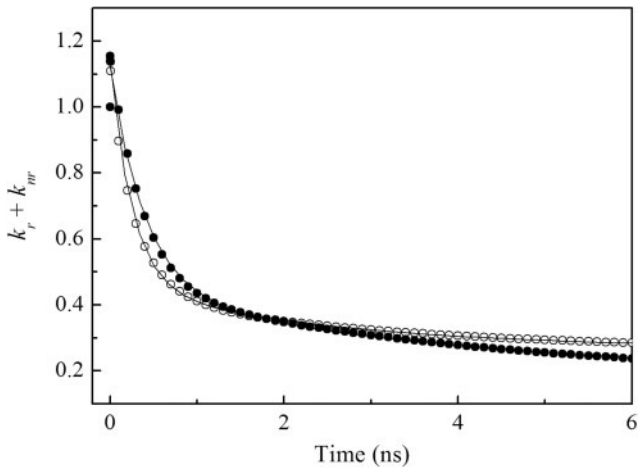

Fig. 6. **Time variation of the sum of the radiative and non-radiative decay rates.** The plots in the graph showed the sum of the radiative and non-radiative decay rates at arbitrary time calculated by using Eq. 5. Open circles, melittin; filled circles, the complex with CaM. These data were fitted by $k_r + k_{nr} = \sum \alpha_{ki} \exp(-t/\tau_{ki}) + k_r(\infty) + k_{nr}(\infty)$shown by solid line.

Table 3. **Decay parameters of the sum of the radiative and non-radiative decay rates.**

	α_{k1}	α_{k2}	τ_{k1} (ns)	τ_{k2} (ns)	$\{k_r(\infty) + k_{nr}(\infty)\}/10^7$ (s^{-1})
Melittin	0.223	0.777	2.48	0.257	26.7
Complex	0.261	0.682	4.10	0.405	17.9

These parameters were obtained by fitting curves shown in Fig. 4 with $k_r + k_{nr} = \sum \alpha_{ki} \exp(-t/\tau_{ki}) + k_r(\infty) + k_{nr}(\infty)$.

(τ_{Nav}) shown in Table 4. Average lifetime of complex was 1.11-fold longer than that of melittin. The time averaged radiative decay rate ($\langle k_r \rangle$) could be calculated by using quantum yield (Φ_s) as follows:

$$\langle k_r \rangle = \frac{\Phi_s}{\tau_{Nav}} \tag{7}$$

We used *N*-acetyl-L-tryptophanamide (NATA) in water as fluorescence standard ($\Phi_{NATA} = 0.13$ and $\tau_{av} = 3.06$) (*4*, *22*). Table 5 showed the time average radiative decay rates of melittin and the complex were about one order smaller than $k_r(\infty) + k_{nr}(\infty)$. This fact demonstrates that time variations of sum of the overall decay rate in melittin and the complex were mostly attributed to non-radiative decay rate. So the limit of overall decay rate ($k_r(\infty) + k_{nr}(\infty)$) shown in Table 2 suggested that Trp residue in melittin was released from some of interactions which caused fluorescence quenching by binding with CaM. The origin of interacting dipole in melittin and the complex with CaM producing dielectric relaxation was difficult to identify in this study because microscopic structure of the complex with CaM has not been determined and there are several candidates involved in dielectric relaxation in protein matrix such as C=O (2.31 D) and N–H (1.31 D) in α-helical configuration, which display the almost same magnitude of dipole moment as water (1.85 D) (*23*, *24*). If water molecule is predominantly involved in the dielectric relaxation, exchanging H_2O for D_2O may change its relaxation rate.

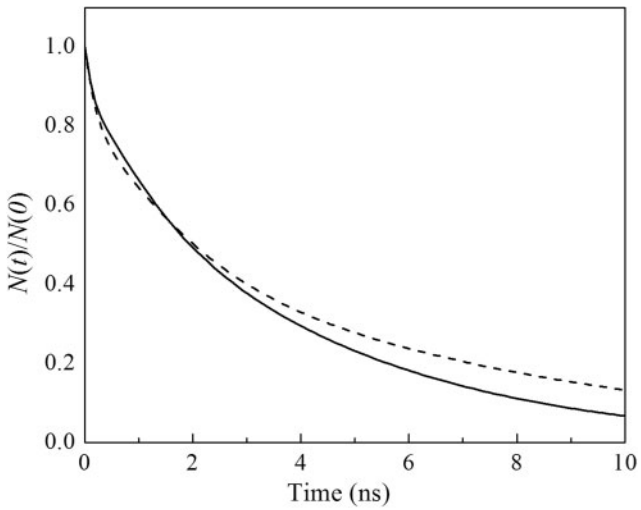

Fig. 7. **Decay curves of excited state fluorophore population.** These curves were calculated by using Eq. 6. These data were fitted by $N(t)/N(0) = \sum \alpha_{Ni} \exp(-t/\tau_{Ni})$. Solid line, melittin; dashed line, the complex with CaM.

Table 4. **Decay parameters of excited state fluorophore population.**

	α_{N1}	α_{N2}	α_{N3}	τ_{N1} (ns)	τ_{N2} (ns)	τ_{N3} (ns)	τ_{Nav} (ns)
Melittin	0.58	0.33	0.09	5.66	1.75	0.09	3.88
Complex	0.56	0.31	0.13	6.83	1.51	0.13	4.31

These parameters were obtained by fitting curves shown in Fig. 5 with $N(t)/N(0) = \sum \alpha_{Ni} \exp(-t/\tau_{Ni})$.

Table 5. **Fluorescence spectroscopic parameters.**

	τ_{Nav} (ns)	Φ_s	$\langle k_r \rangle/10^7$ (s^{-1})
Melittin	3.88	0.105	2.7
Complex	4.31	0.139	3.2
NATA	3.06	0.130	4.2

τ_{Nav} was obtained by $\tau_{Nav} = 1/\int \{k_r(t) + k_{nr}(t)\}dt$ and Φ_s was calculated by $\Phi_s = \frac{F_s}{F_{NATA}} \times \Phi_{NATA}$. $\langle k_r \rangle$ was calculated by Eq. 7.

CONCLUSIONS

We investigated multi-exponential property of fluorescence decay of single-Trp protein on the basis of dielectric relaxation model and applied it to protein–protein interaction study. Though time variation of the centre of gravity showed that the energy difference between relaxed excited state and ground state of melittin and the complex were almost the same, dramatic change of relaxation rate and scale was recognized. We also discussed time variations of sum of radiative and non-radiative decay rates. This also demonstrated notable change of the limit of non-radiative decay rate between melittin and the complex with CaM. Those results proved dielectric relaxation is responsible for multi-exponential

property of fluorescence decay in melittin and the complex.

Understanding the origin of non-radiative process and its relation to excited state energy dissipation, we can elucidate structure–function relationship of proteins.

We are grateful to Prof H. Yoshikawa and Dr Y. Ichiki at Fukuoka Institute of Technology for supporting MALDI-TOF MS spectrometry.

REFERENCES

1. Lakowicz, J.R. (1999) *Principles of Fluorescence Spectroscopy*, 2nd edn, Kluwer Academic/Plenum Publishers, New York
2. Slaughter, B.D., Allen, M.W., Unruh, J.R., Urbauer, R.J.B., and Johnson, C.K. (2004) Single-molecule resonance energy transfer and fluorescence correlation spectroscopy of calmodulin in solution. *J. Phys. Chem. B* **108**, 10388–10397
3. Liu, R., Hu, D., Tin, X., and Lu, H.P. (2006) Revealing two-state protein-protein interactions of calmodulin by single-molecule spectroscopy. *J. Am. Chem. Soc.* **128**, 10034–10042
4. Włodarczyk, J. and Kierdaszuk, B. (2003) Interpretation of fluorescence decays using a power-like model. *Biophys. J.* **85**, 589–598
5. Noronha, M., Lima, J.C., Lamosa, P., Santos, H., Maycock, C., Ventura, R., and Maçanita, A.L. (2004) Intramolecular fluorescence quenching of tyrosine by the peptide α-carbonyl group revisited. *J. Phys. Chem. A* **108**, 2155–2166
6. Pan, C.P. and Barkley, M.D. (2004) Conformational effects on tryptophan fluorescence in cyclic hexapeptides. *Biophys. J.* **86**, 3828–3835
7. Hudson, B.S., Huston, J.M., and S-Campos, G. (1999) A reversible "dark state' mechanism for complexity of the fluorescence of tryptophan in proteins. *J. Phys. Chem. A* **103**, 2227–2234
8. Hellings, M., Maeyer, M.D., Verheyden, S., Hao, Q., Damme, E.J.M.V., Peumans, W.J., and Engelborghs, Y. (2003) The dead-end elimination method, tryptophan rotamers, and fluorescence lifetimes. *Biophys. J.* **85**, 1894–1902
9. Toptygin, D., Gronenborn, A.M., and Brand, L. (2006) Nanosecond relaxation dynamics of protein GB1 identified by the time-dependent red shift in the fluorescence of tryptophan and 5-fluorotryptophan. *J. Phys. Chem. B* **110**, 26292–26302
10. Toptygin, D., Savtchenko, R.S., Meadow, N.D., and Brand, L. (2001) Homogeneous spectrally- and time-resolved fluorescence emission from single-tryptophan mutants of IIA^{Glc} protein. *J. Phys. Chem. B* **105**, 2043–2055
11. Toptygin, D. and Brand, L. (2000) Spectrally- and time-resolved fluorescence emission of indole during solvent relaxation: a quantitative model. *Chem. Phys. Lett.* **322**, 496–502
12. Xu, J., Toptygin, D., Graver, K.J., Albertini, R.A., Savtchenko, R.S., Meadow, N.D., Roseman, S., Callis, P.R., Brand, L., and Knutson, J.R. (2006) Ultrafast fluorescence dynamics of tryptophan in the proteins monellin and IIA^{Glc}. *J. Am. Chem. Soc.* **128**, 1214–1221
13. Lee, A.L., Sharp, K.A., Kranz, J.K., Song, X.J., and Wand, A.J. (2002) Temperature dependence of the internal dynamics of a calmodulin-peptide complex. *Biochemistry* **41**, 13814–13825
14. Yamniuk, A.P. and Vogel, H.J. (2004) Calmodulin's flexibility allows for promiscuity in its interactions with target proteins and peptides. *Mol. Biotechnol.* **27**, 33–58
15. Ishida, H. and Vogel, H.J. (2006) Protein-peptide interaction studies demonstrate the versatility of calmodulin target protein binding. *Protein. Pept. Lett.* **13**, 455–465
16. Bayley, P., Martin, S., Browne, P., and Royer, C. (2003) Time-resolved fluorescence anisotropy studies show domain-specific interactions of calmodulin with IQ target sequences of myosin V. *Eur. Biophys. J.* **32**, 122–127
17. Jurado, L.A., Chockalingam, P.S., and Jarrett, H.W. (1999) Apocalmodulin. *Physiol. Rev.* **79**, 661–682
18. Itakura, M. and Iio, T. (1992) Static and kinetic studies of calmodulin and melittin complex. *J. Biochem.* **112**, 183–191
19. Yazawa, M., Sakuma, M., and Yagi, K. (1980) Calmodulins from muscles of marine invertebrates, scallop and sea anemone: comparison with calmodulins from rabbit skeletal muscle and pig brain. *J. Biochem.* **87**, 1313–1320
20. Fukunaga, Y., Nishimoto, E., Yamashita, K., Otosu, T., and Yamashita, S. (2007) The partially unfolded state of β-momorcharin characterized with steady-state and time-resolved fluorescence studies. *J. Biochem.* **141**, 9–18
21. McKinnon, A.E., Szabo, A.G., and Miller, D.R. (1977) The deconvolution of photoluminescence data. *J. Phys. Chem.* **81**, 1564–1570
22. Sau, A.K., Chen, C.A., Cowan, J.A., Mazumder, S., and Mitra, S. (2001) Steady-state and time-resolved fluorescence studies on wild type and mutant *Chromatium vinosum* high potential iron proteins: holo- and apo-forms. *Biophys. J.* **81**, 2320–2330
23. Takashima, S.J. (2002) Electric dipole moments of globular proteins: measurement and calculation with NMR and X-ray databases. *Non-Cryst. Solids* **305**, 303–310
24. Gregory, J.K., Clary, D.C., Liu, K., Brown, M.G., and Saykally, R.J. (1997) The water dipole moment in water clusters. *Science* **275**, 814–817